Published in final edited form as:
Arterioscler Thromb Vasc Biol. 2009 November ; 29(11): 1730–1736. doi:10.1161/ATVBAHA.109.192963.

Lack of tyrosylprotein sulfotransferase activity in hematopoietic cells drastically attenuates atherosclerosis in *Ldlr*-/- mice

Andrew D. Westmuckett and **Kevin L. Moore**
Cardiovascular Biology Research Program, Oklahoma Medical Research Foundation (A.D.W., K.L.M.), and the Departments of Cell Biology and Medicine, University of Oklahoma Health Sciences Center (K.L.M.), Oklahoma City, Oklahoma

Abstract

Objective—Leukocyte recruitment is a major contributor in the development of atherosclerosis and requires a variety of proteins such as adhesion molecules, chemokines, and chemokine receptors. Several key molecular players implicated in this process are expressed on monocytes and require protein-tyrosine sulfation for optimal function *in vitro*, including human CCR2, CCR5, CX3CR1, and PSGL-1. We therefore hypothesized that protein-tyrosine sulfation in hematopoietic cells plays an important role in the development of atherosclerosis.

Methods and Results—Lethally-irradiated *Ldlr*-/- mice were rescued with hematopoietic progenitors lacking tyrosylprotein sulfotransferase (TPST) activity due to deletion of the *Tpst1* and *Tpst2* genes. TPST deficient progenitors efficiently reconstituted hematopoiesis in *Ldlr*-/- recipients and transplantation had no effect on plasma lipids on a standard or atherogenic diet. However, we observed a substantial reduction in the size of atherosclerotic lesions and the number of macrophages in lesions from hyperlipidemic *Ldlr*-/- recipients transplanted with TPST deficient progenitors compared to wild type progenitors. We also document for the first time that murine Psgl-1 and Cx3cr1 are tyrosine-sulfated.

Conclusions—These data demonstrate that protein-tyrosine sulfation is an important contributor to monocytes/macrophage recruitment and/or retention in a mouse model of atherosclerosis.

Keywords

atherosclerosis; genetically altered mice; protein-tyrosine sulfation

Protein-tyrosine sulfation, a post-translational modification of secretory and membrane proteins is mediated by two Golgi isoenzymes, tyrosylprotein sulfotransferases-1 and -2 (TPST-1 and -2)[1, 2]. TPSTs are broadly expressed in multicellular organisms and catalyze the transfer of a sulfuryl group from 3'-phosphoadenosine 5'-phosphosulfate to the hydroxyl group of peptidyl-tyrosine[3]. Human and mouse TPST-1 are ≈ 96% identical. Human and mouse TPST-2 have a similar degree of identity and are ≈ 67% identical to their TPST-1 counterparts.

Much of the data recognizing the importance of tyrosine sulfation in protein function has been obtained from *in vitro* studies[3-7]. Evidence for the importance of tyrosine sulfation *in vivo* is very limited. Thus, we developed *Tpst1*-/-, *Tpst2*-/- and *Tpst1*-/-; *Tpst2*-/- double knockout (*Tpst* DKO) mice[8-10]. Our studies revealed that both *Tpst1*-/- and *Tpst2*-/- mice are viable and

Corresponding author: Andrew D. Westmuckett, Ph.D., Oklahoma Medical Research Foundation, 825 NE 13th Street, Oklahoma City, OK 73104, Phone: (405) 271-2740, FAX: (405) 271-7417, Andrew-Westmuckett@omrf.org.

Disclosures
Kevin Moore is a co-founder of Siwa Biotech Corporation.

have distinct phenotypes. In part, this is due to differences in substrate specificity of the two isoenzymes[11]. In addition, *Tpst* DKO mice have early postnatal lethality due to pulmonary insufficiency of unknown cause[10]. Together, these studies demonstrate that TPST-1 and TPST-2 have distinct but overlapping function.

The role of tyrosine sulfation in protein function has been demonstrated for a number of proteins[3, 12]. For example, sulfation of platelet gp1bα and factor VIII is required for efficient binding to thrombin[13] and von Willebrand factor[14] respectively, while sulfation of factor V and factor VIII is required for optimal proteolytic processing[15, 16]. In the human system, sulfation of P-selectin glycoprotein ligand-1 (PSGL-1) is required for optimal binding to P- and L-selectin[4]. In addition, sulfation of the N-terminal extracellular domains of certain G-protein coupled receptors, including several chemokine receptors (i.e. CCR2, CCR5, CX3CR1), glycoprotein hormone receptors (i.e. thyroid stimulating hormone), and others is required for optimal ligand binding and ligand-induced responses *in vitro*[3, 5-7, 17]. Mouse orthologs of several of these proteins have been shown to play important roles in mouse models of atherosclerosis, including Psgl-1, Ccr2, Ccr5, and Cx3cr1. Significantly, attenuation of atherosclerosis is observed in *ApoE*-/- mice that are also deficient in Psgl-1, Ccr2, Ccr5, and Cx3cr1[18-22]. However, the importance of tyrosine sulfation in a complex chronic inflammatory disease such as atherosclerosis is unknown.

To explore this question we assessed the development of atherosclerosis in a model in which *Tpst* DKO hematopoietic progenitors were used to reconstitute hematopoiesis in hyperlipidemic *Ldlr*-/- mice. We observed that TPST deficient progenitors reconstituted hematopoiesis in *Ldlr*-/- recipients and that transplantation had no discernible effect on plasma lipids in *Ldlr*-/- recipients fed either a standard or atherogenic diet. However, we observed a substantial reduction in both lesion size and in the number of macrophages in lesions from *Ldlr*-/- recipients transplanted with *Tpst* DKO compared to wild type hematopoietic progenitors.

Methods

Atherosclerosis model

The generation and characterization of *Tpst1*-/-; *Tpst2*-/- double knockout mice in the 129S6 background was described previously [10, 23] and is discussed in detail in Supplemental Material. *Tpst* DKO mice have severely impaired post-natal viability[10]. Therefore, fetal livers were used as the source of hematopoietic progenitors. *Tpst* DKO and wild type fetuses were generated by timed matings of *Tpst1*-/-; *Tpst2*+/- and wild type males and females, respectively. Fetal livers were harvested at E15.5 and single cell suspensions were prepared by passage through 40 μm nylon strainers. Cells were washed in Hank's balanced salt solution (HBSS), 10 mM HEPES, 10% fetal bovine serum and stored at 4°C until transplanted. *Tpst* DKO fetuses were identified by flow cytometry using PSG2, a monoclonal antibody (mAb) that recognizes sulfotyrosine residues in proteins[23] (see Supplemental Methods). Genotypes were confirmed by PCR for the presence of wild type and mutant alleles at the *Tpst1* and *Tpst2* loci[8, 9].

The transplant protocol and timing of experimental endpoints is illustrated in Figure 1. *Ldlr*-/- recipients (8 week old females, B6.129S7-*Ldlr*^{tm1Her}, Jackson Labs) were provided antibiotics in the drinking water (50 mg/L doxycycline, 100 mg/L enrofloxacin) beginning on day -2. On day 0, animals received 6.5 and 5.5 Gray of γ-radiation separated by 4 h and then received 2 × 10^6 fetal liver cells from wild type C57BL/6J, wild type 129S6, or 129S6-*Tpst* DKO fetuses in 200 μl of HBSS, 10 mM HEPES by injection into the retro-orbital venous plexus. These transplant groups are abbreviated as B6-WT→*Ldlr*, 129-WT→*Ldlr*, and 129-*Tpst* DKO→*Ldlr*, respectively. Animals were fed a normal fat diet (Purina Mills #5053) until day

+14 when antibiotics were discontinued and animals were switched to an atherogenic diet (0.15% cholesterol and 21.2% milk fat, Harlan Teklad, #TD88137) for the remaining 16 weeks.

Lipid analysis

Mice were fasted for 6 h and blood collected into aprotinin, EDTA, and gentamicin at final concentrations of 1 μg/ml, 10 mM, 0.2 mg/ml, respectively. Plasma was prepared by centrifugation. Total and HDL cholesterol were measured using the Cholesterol E kit (WAKO Chemicals) and triglycerides measured using the GPO-Trinder triglyceride kit (Sigma). All assays were performed in triplicate.

Blood counts

At 18 weeks post-transplant, animals were anesthetized with Avertin (250 mg/kg, i.p.) and exsanguinated. Blood was collected into EDTA and blood counts were performed using a Hemovet® HV950FS Hematology Analyzer (Drew Scientific).

Lesion analysis

Hearts were perfused with 4% paraformaldehyde for 15 min and then the heart and proximal aorta were removed and fixed for 72 h. Tissues were washed in PBS and embedded in OCT compound and frozen in liquid nitrogen-cooled isopentane. Lesion analysis was performed as previously described[24]. Briefly, serial 10 μm sections through the entire aortic valve and sinus were collected on slides so that each slide contained every tenth section. Slides were stained with oil red O and counterstained with hematoxylin. For each section, lesion area (oil red O reactive area) and the area within the internal elastic lamina were measured from digital images using a digitizing tablet (Model CTE-630BT, Wacom Technology) and ImageJ software. The ratio of lesion area to area within the internal elastic lamina was calculated and averaged over all sections spanning the lesion. The extent of lesion necrosis, defined as the ratio of acellular area to lesion area, was calculated and averaged over 3 mid-valve sections.

Macrophages were quantitated using immunofluorescence microscopy in sections immediately adjacent to those stained with oil red O. Frozen sections were blocked in PBS/3% fish gelatin (Ted Pella Inc.) for 1 h. Macrophages were labeled using 25 μg/ml of the rat anti-mouse monocyte/macrophage mAb MOMA-2 (IgG_{2b}, AbD Serotec) for 1 h. Sections were washed and incubated in 10 μg/ml biotin-conjugated, mouse-adsorbed, rabbit anti-rat IgG (Vector Labs) for 1 h. After washing, sections were incubated in 10 μg/ml Alexa Fluor 488 streptavidin (Invitrogen) for 1 h, washed, rinsed in H_20, and mounted in Vector hard mount containing DAPI. PBS/0.5% gelatin was used for washing and for diluting reagents. Sections stained in parallel using control rat IgG_{2b} mAb (AbD Serotec) revealed minimal non-specific immunofluorescence. Fluorescence images were captured using a Photometrics CoolsnapHQ camera coupled to a Nikon Eclipse TE2000-U microscope. All images were captured at the same magnification, filter, and camera settings and were processed using Metamorph software (v6.1, Molecular Devices).

The number of macrophages in the lesions was determined by counting DAPI-stained nuclei within areas immunoreactive with MOMA-2. Cells per mm^2 were calculated by dividing the number of DAPI-stained nuclei within MOMA-2 positive regions by the area of the MOMA-2 positive region. This area was determined by standardizing equally thresholded images to a 200 × 200 μm calibration square. For each animal, the number of cells per mm^2 was determined on three mid-valve sections collected at 100 μm intervals.

To assess if lesional macrophages were of donor or recipient origin, frozen sections were labeled with MOMA-2 (25 μg/ml) and PSG2 (10 μg/ml) or equivalent concentrations of control antibodies for 1 h followed by biotinylated rabbit anti-rat IgG (10 μg/ml) for 30 min and finally,

10 μg/ml streptavidin-CY5 (eBioscience) and anti-human IgG-FITC (10 μg/ml) for 30 min. Sections were mounted and images captured as above.

Results

Lesion analysis

Ldlr-/- recipients were transplanted with fetal liver hematopoietic progenitors from either *Tpst* DKO or wild type fetuses in the 129S6 background or wild type C57BL/6J fetuses. Eighteen weeks after transplant, atherosclerotic lesions were evident in all transplant groups. In control B6-WT→*Ldlr* and 129-WT→*Ldlr* animals, the lesions encompassed 24.2 ± 3.0% (mean ± S.E.M., $n = 6$) and 19.2 ± 2.7% ($n = 10$) of the area within the internal elastic lamina, respectively (Fig. 2A and Supplemental Fig. I). In contrast, the lesions in 129-*Tpst* DKO→*Ldlr* animals encompassed only 6.2 ± 0.9 % ($n = 10$) of the area within the internal elastic lamina, a ≈ 3-fold reduction in lesion size (Fig. 2B). Lesion size in the three groups was significantly different ($p < 0.0001$, one-way ANOVA). Post-hoc *t* testing showed that lesions in the 129-*Tpst* DKO→*Ldlr* group were smaller compared to both the B6-WT→*Ldlr* ($p < 0.0001$) and 129-WT→*Ldlr* ($p = 0.0003$) groups. However, lesion size was not different between B6-WT→*Ldlr* and 129-WT→*Ldlr* mice ($p = 0.25$).

We also quantitated the extent of necrosis within the atherosclerotic lesions. Necrosis was evident in lesions from all transplanted groups and the total necrotic area was reduced in 129-*Tpst* DKO→*Ldlr* lesions compared to the control groups. However, there were no statistical differences in the ratio of necrotic area to lesion area between transplant groups (Fig. 2C) ($p = 0.32$, one-way ANOVA). The number of lesional macrophages was determined in 3 mid-valve sections from five animals in each experimental group at 18 weeks post-transplant. Accumulation of macrophages was evident in all transplanted groups (Fig. 2E). In control B6-WT→*Ldlr* and 129-WT→*Ldlr* animals, the number of macrophages in lesions was 4,558 ± 917 and 5,447 ± 758 cells/mm^2, respectively (mean ± S.E.M.). In contrast, we observed only 2,232 ± 168 cells/mm^2 in the lesions in 129-*Tpst* DKO→*Ldlr* animals (Fig. 2D). The number of macrophages in the three groups was statistically different ($p = 0.018$, one-way ANOVA). Post-hoc *t* testing showed that the number of macrophages in the 129-*Tpst* DKO→*Ldlr* group was smaller compared to the B6-WT→*Ldlr* ($p = 0.0372$) and the 129-WT→*Ldlr* group ($p = 0.0033$) group. However, the number of macrophages was not different between B6-WT→*Ldlr* and 129-WT→*Ldlr* mice ($p = 0.48$).

To assess if the attenuation of lesion development was specific for the aortic root, *en face* oil red O staining of the abdominal aortas from four animals in each transplant group was performed focusing on the ostia of the intercostal arteries. We observed a similar degree of attenuation of lesion development in the 129-*Tpst* DKO→*Ldlr* group compared to the control groups as observed in the aortic root (Supplemental Fig. III).

Lipid analysis

The impact of the transplants on lipid metabolism was assessed by measuring total cholesterol, HDL cholesterol, and triglyceride levels at 2 weeks post-transplant while mice were on a normal chow diet and then again at 6 and 14 weeks post-transplant, while on a atherogenic diet (Table 1). No statistical differences were observed between the groups at 2 weeks post-transplant while on normal chow. As anticipated, total cholesterol, HDL cholesterol, and triglyceride levels increased in all three groups after 4 and 12 weeks on the atherogenic diet. However, there were still no statistical differences between groups.

Hematopoietic reconstitution

Blood counts were performed 18 weeks post-transplant. Total leukocyte, lymphocyte, monocyte, and platelet counts were not statistically significant different between the transplant groups (Supplemental Table I). However, neutrophil and erythrocyte counts were statistically different as assessed by one-way ANOVA. Post-hoc *t* testing showed that neutrophil counts were higher in the 129-WT→*Ldlr* group compared to B6-WT→*Ldlr* groups ($p = 0.022$). In addition, erythrocyte counts were higher in the B6-WT→*Ldlr* compared to the 129-*Tpst* DKO→*Ldlr* ($p = 0.003$). Nevertheless, all parameters were within the normal range.

To assess the efficiency of reconstitution of *Tpst* DKO hematopoiesis in *Ldlr*-/- mice, the percentage of circulating PSG2 positive leukocytes was determined at 18 weeks post-transplant. Analysis of the leukocyte population from 129-WT→*Ldlr* mice showed that virtually all the circulating leukocytes were PSG2 positive (Fig. 3, top). However, fluorescence (FL1) histograms of cells stained with isotype control mAb and PSG2 are not completely resolved. Thus, the valley between the two FL1 histograms was used to define the FL1 threshold for quantitating the percentage of PSG2 positive cells in 129-*Tpst* DKO→*Ldlr* mice (Fig. 3, bottom). It should be noted that this definition might underestimate the degree of donor hematopoiesis in mice transplanted with *Tpst* DKO progenitors. Nevertheless, 82.4 ± 1.9% (mean ± S.E.M., $n = 10$) of the total leukocytes displayed a $PSG2^{lo}$ phenotype and thus were of donor origin. By the same criteria, 92.9 ± 1.1 (mean ± S.E.M., $n = 10$) of the total leukocytes in 129-WT→*Ldlr* mice were $PSG2^{hi}$. Taken together, these data confirm efficient reconstitution of *Tpst* DKO hematopoiesis in the *Ldlr*-/- recipients at the time of lesion analysis.

To assess if the macrophages in the lesions in 129-*Tpst* DKO→*Ldlr* mice were donor or recipient in origin, immunofluorescence staining was performed using MOMA-2 and PSG2 antibodies. We observed clear co-localization of MOMA-2 and PSG2 staining in 129-*Tpst* DKO→*Ldlr* lesions (Fig. 4) indicating that some of the macrophages in these lesions were of recipient and not donor origin.

Psgl-1 and chemokine receptor expression

To assess if the absence of TPSTs in hematopoietic cells affects surface expression of Psgl-1 and a panel of chemokine receptors we examined peripheral blood leukocyte in B6.SJL mice ($CD45.1^+$) transplanted with 15.5 dpc fetal liver cells from *Tpst* DKO mice ($CD45.2^+$) or wild type 129S6 mice by flow cytometry. In three independent comparisons 20-24 weeks post-transplant, surface expression of Psgl-1, Ccr5, and Cx3cr1 was indistinguishable in the 129-*Tpst* DKO→B6.SJL and 129-WT→B6.SJL groups (Supplemental Fig. IIA). At the time of analysis, all recipients had normal blood counts and 90-95% of circulating leukocyte were of donor ($CD45.2^+$) origin (data not shown). We also examined thymocytes from a rare 2-week old *Tpst* DKO survivor and a sex- and age-matched wild type mouse. We observed no differences in the expression of Psgl-1, Ccr6, Ccr7, D6, Cxcr2, and Cxcr4 (Supplemental Fig. IIB).

Sulfotyrosine analysis

It is widely assumed that mouse Psgl-1 and many chemokine receptors are tyrosine-sulfated like their human counterparts. However, this has never been experimentally verified. To address the question, a direct biochemical analysis of metabolically labeled, purified native mouse Psgl-1 and recombinant mouse Cx3cr1 expressed in mouse pre-B L1.2 cells was performed as described in Supplemental Materials. This analysis unambiguously demonstrates that both molecules are tyrosine-sulfated (Fig. 5).

Discussion

Atherosclerosis is a chronic inflammatory disease of the arterial wall initiated by injury of the vascular endothelium leading to endothelial dysfunction and subsequent intramural accumulation of oxidized LDL[25-28]. This is followed by the elaboration of signaling molecules and induction of adhesion receptors that promote recruitment of monocytes into developing lesions, which subsequently mature into lipid-laden foam cells. A compelling body of evidence indicates that recruitment of monocytes is a dominant factor in the initiation and progression of atherosclerosis[29]. Genetic studies in mice indicate that Ccr2, Ccr5, Cx3cr1, and the adhesion molecule Psgl-1, that are all expressed on monocytes, are pro-atherogenic and play important roles in monocyte recruitment in atherosclerosis[18-22, 30, 31]. Furthermore, *in vitro* studies have shown that human CCR2B, CCR5, CX3CR1, and PSGL-1 contain sulfotyrosine residues that are required for optimal function *in vitro*[4-7]. However, at present it is not known if these proteins are sulfated in the mouse system or if sulfation of these proteins is important for their optimal function *in vivo*.

Based on these data, we examined the effect of hematopoietic deficiency of TPST activity on the development of atherosclerosis in a model in which *Tpst* DKO hematopoietic progenitor cells were used to reconstitute hematopoiesis in *Ldlr*-/- mice. We observed a 68% reduction in the size of aortic root lesions in recipients transplanted with TPST deficient progenitors compared to 129S6 wild type controls. The reduction in lesion size was accompanied by a 2-3 fold-reduction in the number of lesional macrophages. As expected, attenuated lesions in 129-*Tpst* DKO→*Ldlr* animals contained smaller necrotic areas. However, no differences in the ratio of necrotic area to lesion size were apparent between the experimental and control groups. This suggests that while TPST deficiency in macrophages attenuates monocyte/macrophage recruitment and/or retention, it does not perturb phagocytic clearance of apoptotic/necrotic cells.

To address potential mechanism(s) for the reduction in lesion size, factors known to be important in lesion development and/or progression were assessed. Lipid metabolism and especially LDL cholesterol levels are directly correlated with development of atherosclerosis. However, we observed no differences in cholesterol or triglyceride levels between the experimental groups. Thus, TPST deficiency in the hematopoietic compartment does not affect overall lipid homeostasis in the *Ldlr*-/- recipients and that the reduction in lesion size was not due to reduced exposure of the endothelium to plasma-derived lipids. Monocyte recruitment is the major cellular event to influence lesion progression and the level of circulating monocytes can directly impact lesion development[29]. However, we observed no differences in monocyte counts between the experimental and control groups at 18 weeks post-transplant. Reduced lesion size in 129-*Tpst* DKO→*Ldlr* mice may be due to reduced expression of chemokine receptors and/or adhesion molecules on TPST-deficient hematopoietic cells resulting in decreased recruitment of monocytes into developing lesions. However, we observed that expression of a panel of chemokine receptors and Psgl-1 on *Tpst* DKO hematopoietic cells was normal. This finding is consistent with previous observations that inhibition of tyrosine sulfation has no impact on the secretion or surface expression of a variety of tyrosine-sulfated proteins, including chemokine receptors[3, 5].

In our experimental group, *Tpst* DKO fetal liver cells from 129S6 donors were used to reconstitute hematopoiesis in *Ldlr*-/- recipients in the B6 background. However, no difference in any experimental endpoint was observed between the controls in which wild type 129S6 or C57BL/6J mice were used as donors. Therefore, the reduction in lesion size in the 129-*Tpst* DKO6*Ldlr* group is not related to the difference in genetic background between donor and recipient.

In this study, we used the anti-sulfotyrosine mAb PSG2 to identify *Tpst* DKO donor fetuses and to assess the degree of chimerism in mice transplanted with *Tpst* DKO progenitors. In the 129-*Tpst* DKO→*Ldlr* mice at 18 weeks post-transplant, we found that on average ≈ 82% of the total leukocytes were $PSG2^{lo}$ and thus were of donor origin. This led us to ask if the lesional macrophages in these mice were donor or recipient in origin. Immunofluorescence staining showed co-localization of PSG2 and MOMA-2 staining in 129-*Tpst* DKO→*Ldlr* lesions. This indicates that at least some of the lesion development observed in 129-*Tpst* DKO→*Ldlr* mice may be due to residual recipient hematopoiesis suggesting that lesion development might have been further attenuated if a higher level of chimerism had been achieved. Alternatively, co-localization of PSG2 and MOMA-2 in lesions may be a reflection of close association of sulfated plasma proteins or membrane microparticles derived from the recipient. It is also possible, but very unlikely, that this co-localization reflects in-trans sulfation of donor macrophage proteins by TPSTs derived from recipient cells.

The 68% reduction in aortic root lesion area we observed is greater than that reported in *ApoE*-/-; *Cx3cr1*-/- (32%)[22], *ApoE*-/-; *Selplg*-/- (≈ 40%)[18], and *ApoE*-/-; *Ccr5*-/- double knockouts (≈ 50%)[21], but comparable to that observed in *ApoE*-/-; *Ccr2*-/- double knockouts (≈ 60%)[19, 20]. However, the relative impact that defective sulfation of these proteins has in lesion attenuation is unclear. Nevertheless, it is reasonable to conclude that the dramatic reduction in aortic root lesion area observed is due to defective sulfation of multiple proteins involved in monocyte recruitment and/or retention, including Psgl-1, Cx3cr1 (Fig. 5) as well as Ccr2, Ccr5 and other proteins yet to be identified.

Our findings suggest that strategies for treatment and prevention of atherosclerosis might be developed based either on drugs that inhibit the interaction between specific tyrosine-sulfated proteins and their cognate ligand(s) or ones that inhibit TPST activity. Targeting a specific receptor/ligand interaction might be favored if that interaction plays the dominant role in development of atherosclerosis. However, as discussed above, current data argues that the reduction in atherosclerosis we observe is due to defective sulfation of multiple proteins. In this circumstance, inhibition of TPST activity may be the preferred approach. However, potential off-target effects may limit the viability of this approach given the number of tyrosine-sulfated proteins both known and unknown.

In conclusion, post-translational tyrosine sulfation of protein(s) in hematopoietic cells has a major impact on the development of atherosclerosis in hyperlipidemic *Ldlr*-/- mice. Our findings represent the first direct evidence that protein-tyrosine sulfation plays a key role in the development of a common and clinically important inflammatory disorder.

Supplementary Material

Refer to Web version on PubMed Central for supplementary material.

Acknowledgments

Sources of Funding

This work was supported by Grant HRO7-101 from the Oklahoma Center for the Advancement of Science and Technology (A.D.W.) and NIH Grants HD056022 and HL074015 (K.L.M.).

References

1. Ouyang YB, Lane WS, Moore KL. Tyrosylprotein sulfotransferase: Purification and molecular cloning of an enzyme that catalyzes tyrosine *O*-sulfation, a common posttranslational modification of eukaryotic proteins. Proc Natl Acad Sci U S A 1998;95:2896–2901. [PubMed: 9501187]

2. Ouyang YB, Moore KL. Molecular cloning and expression of human and mouse tyrosylprotein sulfotransferase-2 and a tyrosylprotein sulfotransferase homologue in *Caenorhabditis elegans*. J Biol Chem 1998;273:24770–24774. [PubMed: 9733778]
3. Moore KL. The biology and enzymology of protein tyrosine *O*-sulfation. J Biol Chem 2003;278:24243–24246. [PubMed: 12730193]
4. Wilkins PP, Moore KL, McEver RP, Cummings RD. Tyrosine sulfation of P-selectin glycoprotein ligand-1 is required for high affinity binding to P-selectin. J Biol Chem 1995;270:22677–22680. [PubMed: 7559387]
5. Farzan M, Mirzabekov T, Kolchinsky P, Wyatt R, Cayabyab M, Gerard NP, Gerard C, Sodroski J, Choe H. Tyrosine sulfation of the amino terminus of CCR5 facilitates HIV-1 entry. Cell 1999;96:667–676. [PubMed: 10089882]
6. Fong AM, Alam SM, Imai T, Haribabu B, Patel DD. CX3CR1 tyrosine sulfation enhances fractalkine-induced cell adhesion. J Biol Chem 2002;277:19418–19423. [PubMed: 11909868]
7. Preobrazhensky AA, Dragan S, Kawano T, Gavrilin MA, Gulina IV, Chakravarty L, Kolattukudy PE. Monocyte chemotactic protein-1 receptor CCR2B is a glycoprotein that has tyrosine sulfation in a conserved extracellular N-terminal region. J Immunol 2000;165:5295–5303. [PubMed: 11046064]
8. Ouyang YB, Crawley JTB, Aston CE, Moore KL. Reduced body weight and increased postimplantation fetal death in tyrosylprotein sulfotransferase-1-deficient mice. J Biol Chem 2002;277:23781–23787. [PubMed: 11964405]
9. Borghei A, Ouyang YB, Westmuckett AD, Marcello MR, Landel CP, Evans JP, Moore KL. Targeted disruption of tyrosylprotein sulfotransferase-2, an enzyme that catalyzes post-translational protein tyrosine O-sulfation, causes male infertility. J Biol Chem 2006;281:9423–9431. [PubMed: 16469738]
10. Westmuckett AD, Hoffhines AJ, Borghei A, Moore KL. Early postnatal pulmonary failure and primary hypothyroidism in mice with combined TPST-1 and TPST-2 deficiency. Gen Comp Endocrinol 2008;156:145–153. [PubMed: 18243191]
11. Hoffhines AJ, Jen CH, Leary JA, Moore KL. Tyrosylprotein sulfotransferase-2 expression is required for sulfation of RNase9 and Mfge8 *in vivo*. J Biol Chem 2009;284:3096–3105. [PubMed: 19047058]
12. Kehoe JW, Bertozzi CR. Tyrosine sulfation: a modulator of extracellular protein-protein interactions. Chem Biol 2000;7:R57–61. [PubMed: 10712936]
13. Marchese P, Murata M, Mazzucato M, Pradella P, De Marco L, Ware J, Ruggeri ZM. Identification of three tyrosine residues of glycoprotein Ibα with distinct roles in von Willebrand factor and α-thrombin binding. J Biol Chem 1995;270:9571–9578. [PubMed: 7721887]
14. Leyte A, van Schijndel HB, Niehrs C, Huttner WB, Verbeet MP, Mertens K, van Mourik JA. Sulfation of Tyr^{1680} of human blood coagulation factor VIII is essential for the interaction of factor VIII with von Willebrand factor. J Biol Chem 1991;266:740–746. [PubMed: 1898735]
15. Pittman DD, Wang JH, Kaufman RJ. Identification and functional importance of tyrosine sulfate within recombinant Factor VIII. Biochemistry 1992;31:3315–3325. [PubMed: 1554716]
16. Pittman DD, Tomkinson KN, Michnick D, Selighsohn U, Kaufman RJ. Posttranslational sulfation of factor V is required for efficient thrombin cleavage and activation and for full procoagulant activity. Biochemistry 1994;33:6952–6959. [PubMed: 8204629]
17. Choe H, Farzan M. Chapter 7. Tyrosine sulfation of HIV-1 coreceptors and other chemokine receptors. Methods Enzymol 2009;461:147–170. [PubMed: 19480918]
18. An G, Wang H, Tang R, Yago T, McDaniel JM, McGee S, Huo Y, Xia L. P-selectin glycoprotein ligand-1 is highly expressed on Ly-$6C^{hi}$ monocytes and a major determinant for Ly-$6C^{hi}$ monocyte recruitment to sites of atherosclerosis in mice. Circulation 2008;117:3227–3237. [PubMed: 18519846]
19. Boring L, Gosling J, Cleary M, Charo IF. Decreased lesion formation in CCR2-/- mice reveals a role for chemokines in the initiation of atherosclerosis. Nature 1998;394:894–897. [PubMed: 9732872]
20. Dawson TC, Kuziel WA, Osahar TA, Maeda N. Absence of CC chemokine receptor-2 reduces atherosclerosis in apolipoprotein E-deficient mice. Atherosclerosis 1999;143:205–211. [PubMed: 10208497]
21. Braunersreuther V, Zernecke A, Arnaud C, Liehn EA, Steffens S, Shagdarsuren E, Bidzhekov K, Burger F, Pelli G, Luckow B, Mach F, Weber C. Ccr5 but not Ccr1 deficiency reduces development

of diet-induced atherosclerosis in mice. Arterioscler Thromb Vasc Biol 2007;27:373–379. [PubMed: 17138939]

22. Lesnik P, Haskell CA, Charo IF. Decreased atherosclerosis in CX3CR1-/- mice reveals a role for fractalkine in atherogenesis. J Clin Invest 2003;111:333–340. [PubMed: 12569158]
23. Hoffhines AJ, Damoc E, Bridges KG, Leary JA, Moore KL. Detection and purification of tyrosine-sulfated proteins using a novel anti-sulfotyrosine monoclonal antibody. J Biol Chem 2006;281:37877–37887. [PubMed: 17046811]
24. Paigen B, Morrow A, Holmes PA, Mitchell D, Williams RA. Quantitative assessment of atherosclerotic lesions in mice. Atherosclerosis 1987;68:231–240. [PubMed: 3426656]
25. Ross R. Atherosclerosis - An inflammatory disease. N Engl J Med 1999;340:115–126. [PubMed: 9887164]
26. Libby P. Inflammation in atherosclerosis. Nature 2002;420:868–874. [PubMed: 12490960]
27. Barlic J, Murphy PM. Chemokine regulation of atherosclerosis. J Leukoc Biol 2007;82:226–236. [PubMed: 17329566]
28. Galkina E, Ley K. Vascular adhesion molecules in atherosclerosis. Arterioscler Thromb Vasc Biol 2007;27:2292–2301. [PubMed: 17673705]
29. Weber C, Zernecke A, Libby P. The multifaceted contributions of leukocyte subsets to atherosclerosis: Lessons from mouse models. Nat Rev Immunol 2008;8:802–815. [PubMed: 18825131]
30. Guo J, Van Eck M, Twisk J, Maeda N, Benson GM, Groot PH, Van Berkel TJ. Transplantation of monocyte CC-chemokine receptor 2-deficient bone marrow into ApoE3- Leiden mice inhibits atherogenesis. Arterioscler Thromb Vasc Biol 2003;23:447–453. [PubMed: 12615695]
31. Combadiere C, Potteaux S, Gao JL, Esposito B, Casanova S, Lee EJ, Debre P, Tedgui A, Murphy PM, Mallat Z. Decreased atherosclerotic lesion formation in CX3CR1/apolipoprotein E double knockout mice. Circulation 2003;107:1009–1016. [PubMed: 12600915]

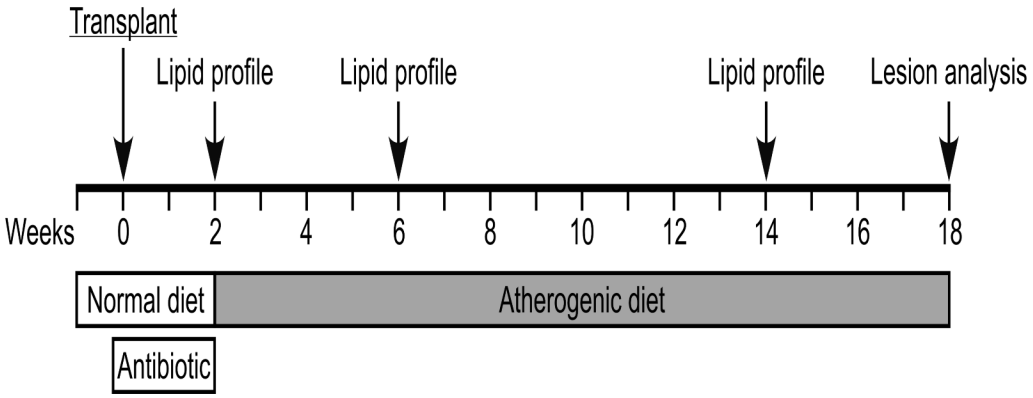

Figure 1.
Transplant protocol.

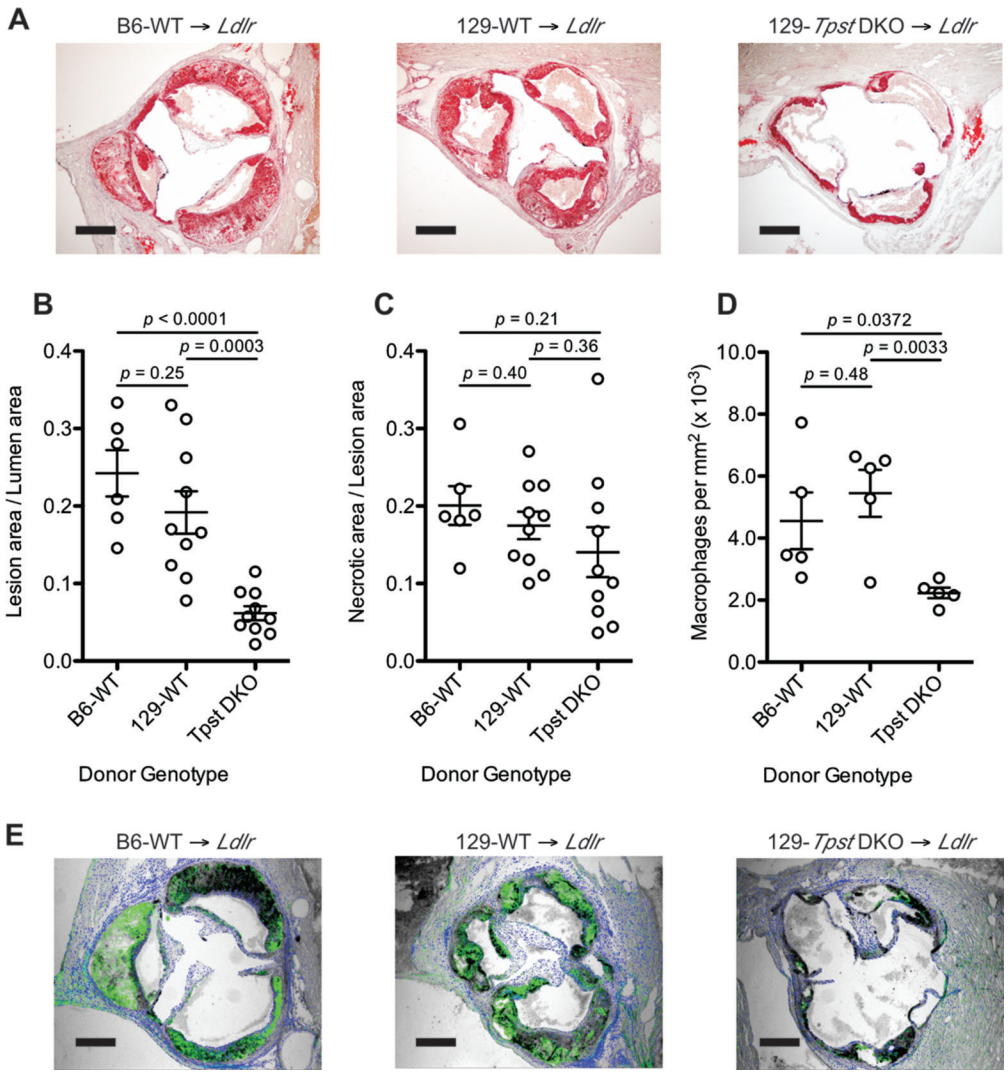

Figure 2.

Lesion analysis. (A) Aortic valves from B6-WT→*Ldlr* (left), 129-WT→*Ldlr* (middle) and 129-*Tpst* DKO→*Ldlr* (right) animals were sectioned at 100 μm intervals spanning the entire lesion (See Supplemental Fig. I) and stained with oil red O. The mid-valve sections shown represent lesions nearest to the mean lesion size for each transplant group. (B) The ratio of the lesion area to the area within the internal elastic lamina was calculated and averaged over the entire lesion. Mean ± S.E.M. (n = 10). (C) Necrotic area was averaged over 3 mid-valve sections. Mean ± S.E.M. (n = 10). (D) Lesional macrophages were quantitated using immunofluorescence microscopy on 3 mid-valve sections adjacent to those used to quantitate lesion size. Mean ± S.E.M. (n = 5). Datasets were subjected to one-way ANOVA and statistical differences between individual groups were assessed by post-hoc testing using a Student's two-tailed t test with unequal sample variance. (E) Representative images of immunofluorescence analyses used to quantitate macrophages in lesions from B6-WT→*Ldlr* (left), 129-WT→*Ldlr* (middle) and 129-*Tpst* DKO→*Ldlr* (right) animals. Macrophages (green) and nuclei (blue) were identified using the MOMA-2 and DAPI, respectively. Bars = 400 μm.

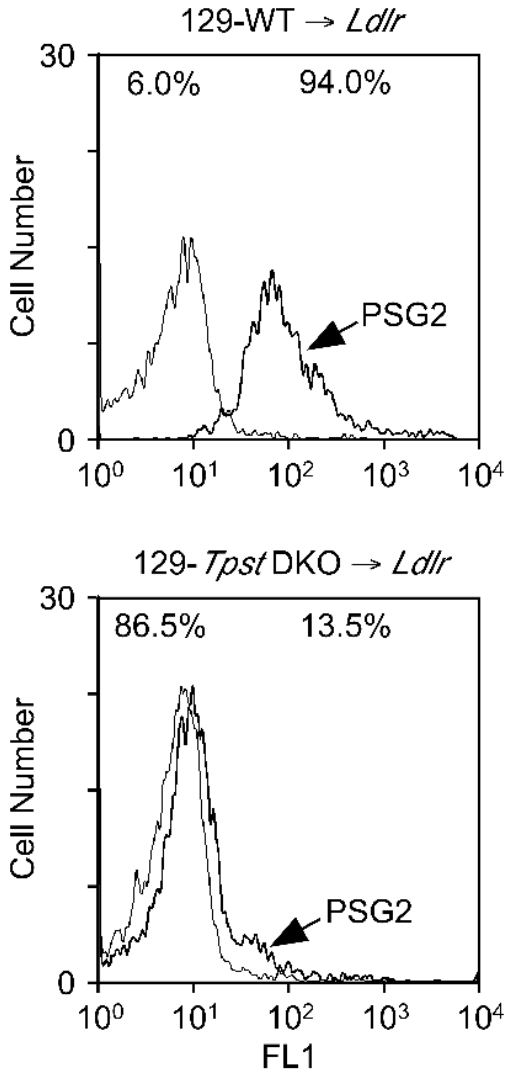

Figure 3.

Quantitation of donor hematopoiesis. The percentage of PSG2 positive peripheral blood leukocytes was determined in 129-WT→*Ldlr* (top) and 129-*Tpst* DKO→*Ldlr* (bottom) animals 18 weeks post-transplant. The FLI threshold defining PSG2 positive cells was taken as the valley between the isotype control and PSG2 FL1 histograms in 129-WT→*Ldlr* cells and is indicated by the vertical line. Percentages of PSG2 positive and negative cells are indicated.

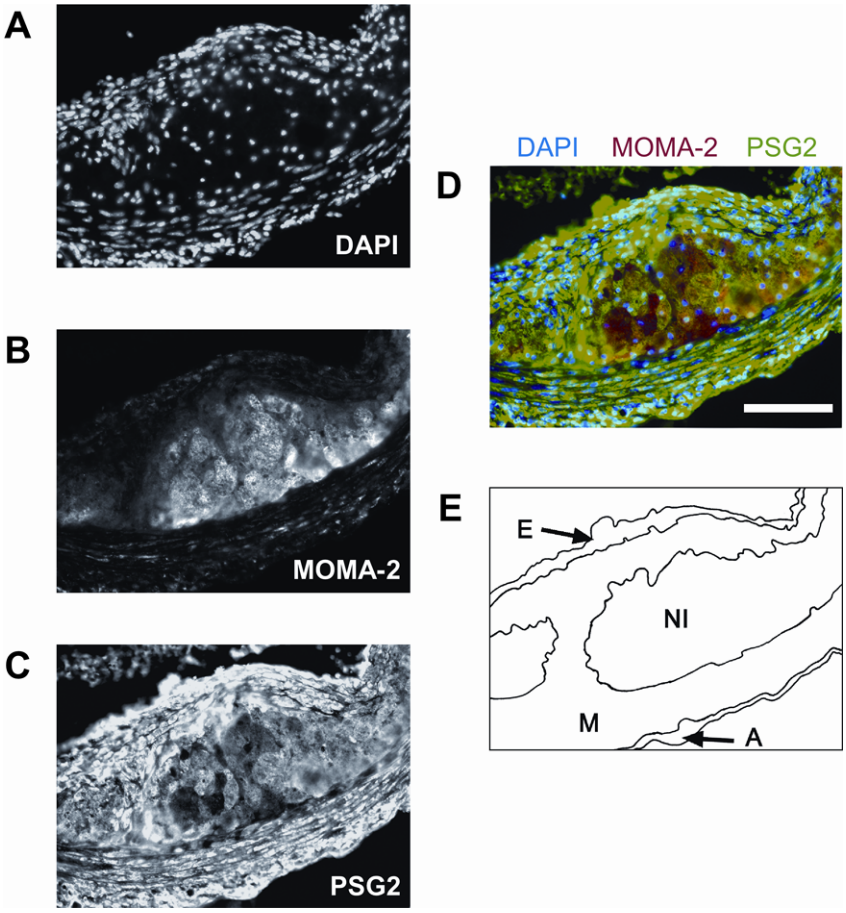

Figure 4.
Immunofluorescence staining of lesional macrophages. A representative lesion from a 129-*Tpst* DKO→*Ldlr* mouse at 18 wks post-transplant stained with DAPI (A), the macrophage specific MOMA-2 mAb (B), and the anti-sulfotyrosine PSG2 (C). D, Merged pseudocolor image. DAPI (blue), MOMA-2 (red), and PSG2 (green). Red/green emission overlap = orange/yellow. E, Diagrammatic representation of the image shown in panel D. E = endothelium, NI = neointima, M = media, and A = adventitia. Bar = 200 μm.

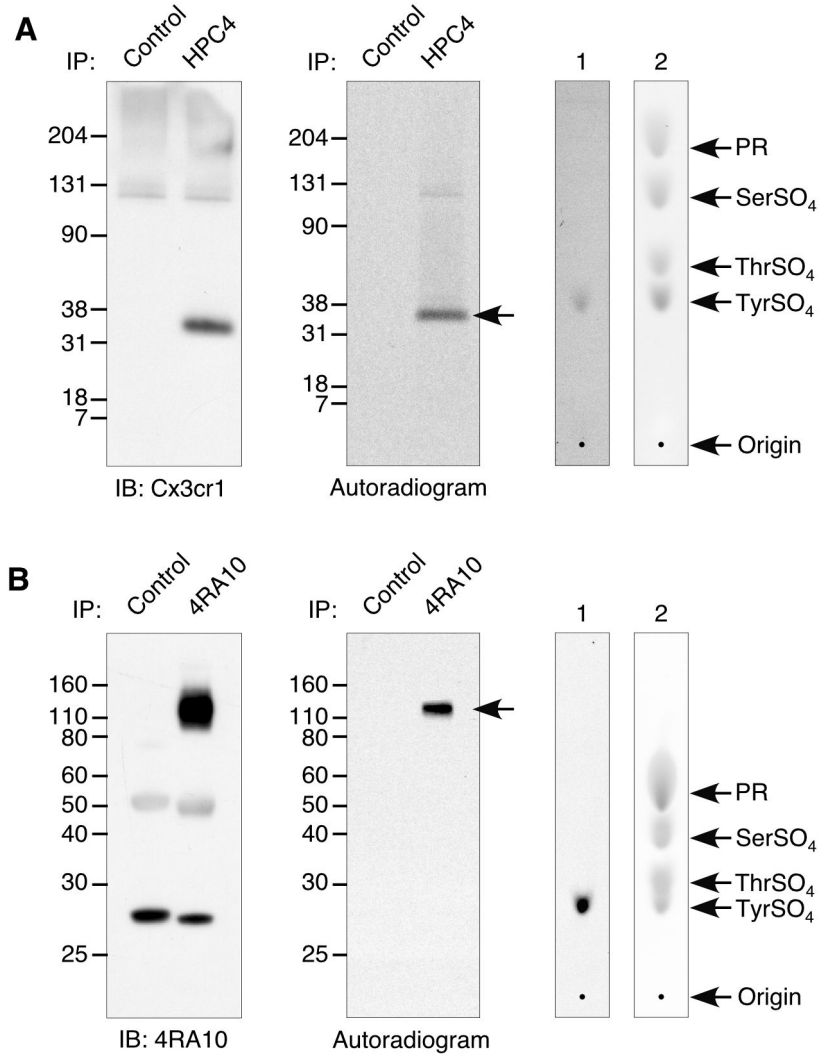

Figure 5.

Sulfotyrosine analysis of Psgl-1 and Cx3cr1. Murine L1.2 pre-B cells transfected with HPC4-tagged mouse Cx3cr1 (A) or bone marrow cells from wild type 129S6 mice (B) were metabolically labeled and Cx3cr1 and Psgl-1 immunoprecipitated using HPC4 or 4RA10, respectively, or isotype control mAbs. Immunoprecipitates were electrophoresed under non-reducing (Cx3cr1) and reducing conditions (Psgl-1) and electroblotted onto PVDF membranes. Membranes were immunoblotted (left panels) or subjected to autoradiography (middle panels). Bands (arrows) were excised, subjected to alkaline hydrolysis and hydrolysates were subjected to thin layer electrophoresis (right panels). Plates were exposed to film to reveal radiolabeled sulfoamino acids (lanes 1) and sprayed with ninhydrin to reveal internal sulfoamino acid standards (lanes 2).

TABLE 1

Lipid Analysis.

	Total cholesterol (mg/dL)			HDL cholesterol (mg/dL)			Triglycerides (mg/dL)		
Donor Genotype	**2 wk**	**6 wk**	**14 wk**	**2 wk**	**6 wk**	**14 wk**	**2 wk**	**6 wk**	**14 wk**
B6-WT	136±7	519±59	693±46	52±1	82±10	77±8	80±9	152±13	187±18
129-WT	133±8	650±66	623±52	48±3	69±8	63±8	74±11	184±9	185±15
129-*Tpst* DKO	137±5	549±69	633±46	49±2	64±6	57±5	73±7	183±24	149±11
ANOVA	0.921	0.343	0.545	0.477	0.261	0.141	0.832	0.307	0.147

Fasting plasma total cholesterol, HDL cholesterol, and triglycerides were determined 2 weeks post-transplant while mice were on normal chow and 6 and 14 weeks post-transplant, while on an atherogenic diet. Mean ± S.E.M. (n = 10) of assays performed in triplicate. Statistical significances between the three experimental groups at each time point were determined by single factor ANOVA.